frontiers | Frontiers in Materials

TYPE Original Research
PUBLISHED 25 August 2022
DOI 10.3389/fmats.2022.969188

Check for updates

OPEN ACCESS

EDITED BY
Yao Shuai,
University of Electronic Science and Technology of China, China

REVIEWED BY
Michael Hoffmann,
University of California, Berkeley, United States
Hong-Sub Lee,
Kangwon National University, South Korea

*CORRESPONDENCE
Shiva Asapu,
sasapu@umass.edu
J. J. Yang,
jjoshuay@usc.edu

SPECIALTY SECTION
This article was submitted to Semiconducting Materials and Devices, a section of the journal Frontiers in Materials

RECEIVED 14 June 2022
ACCEPTED 12 July 2022
PUBLISHED 25 August 2022

CITATION
Asapu S, Pagaduan JN, Zhuo Y, Moon T, Midya R, Gao D, Lee J, Wu Q, Barnell M, Ganguli S, Katsumata R, Chen Y, Xia Q and Yang JJ (2022), Large remnant polarization and great reliability characteristics in W/HZO/W ferroelectric capacitors.
Front. Mater. 9:969188.
doi: 10.3389/fmats.2022.969188

Large remnant polarization and great reliability characteristics in W/HZO/W ferroelectric capacitors

Shiva Asapu[1]*, James Nicolas Pagaduan[2], Ye Zhuo[3], Taehwan Moon[4], Rivu Midya[1], Dawei Gao[5], Jungmin Lee[5], Qing Wu[6], Mark Barnell[6], Sabyasachi Ganguli[7], Reika Katsumata[2], Yong Chen[5], Qiangfei Xia[1] and J. Joshua Yang[1,3]*

[1]Department of Electrical and Computer Engineering, University of Massachusetts, Amherst, MA, United States, [2]Department of Polymer Science and Engineering, University of Massachusetts, Amherst, MA, United States, [3]Department of Electrical and Computer Engineering, University of Southern California, Los Angeles, CA, United States, [4]Samsung Advanced Institute of Technology, Gyeonggi-do, South Korea, [5]Department of Mechanical and Aerospace Engineering, University of California, Los Angeles, Los Angeles, CA, United States, [6]Air Force Research Laboratory, Information Directorate, Rome, NY, United States, [7]Air Force Research Laboratory, Materials and Manufacturing Directorate, Wright - Patterson Air Force Base, Dayton, OH, United States

In this work, the effect of rapid thermal annealing (RTA) temperature on the ferroelectric polarization in zirconium-doped hafnium oxide (HZO) was studied. To maximize remnant polarization ($2P_r$), in-plane tensile stress was induced by tungsten electrodes under optimal RTA temperatures. We observed an increase in $2P_r$ with RTA temperature, likely due to an increased proportion of the polar ferroelectric phase in HZO. The HZO capacitors annealed at 400°C did not exhibit any ferroelectric behavior, whereas the HZO capacitors annealed at 800°C became highly leaky and shorted for voltages above 1 V. On the other hand, annealing at 700 °C produced HZO capacitors with a record-high $2P_r$ of $\sim 64\ \mu C\ cm^{-2}$ at a relatively high frequency of 111 kHz. These ferroelectric capacitors have also demonstrated impressive endurance and retention characteristics, which will greatly benefit neuromorphic computing applications.

KEYWORDS

ferroelectric switching, large remnant polarization, hafnium-zirconium oxide, tungsten, rapid thermal annealing

Introduction

Ever since the first report of ferroelectricity in hafnium oxide (HfO_2) in 2011 (Böscke et al., 2011), considerable efforts have been made to elucidate the origins of ferroelectricity and enhance its performance for emerging applications.

The excellent compatibility of HfO_2 with the complementary metal-oxide-semiconductor (CMOS) process and its suitability as a popular high-*k* gate dielectric has rapidly enabled applications such as ferroelectric random-access memories (FeRAMs) (Francois et al., 2019; Okuno et al., 2020) and ferroelectric field-effect transistors (FeFETs) (George et al., 2016; Dünkel et al., 2017; Dutta et al., 2020). Specifically, FeFET structure-based devices have found their niche in applications such as neuromorphic computing, where they form the basic unit of neural network circuits that can implement brain-inspired algorithms to solve various problems (Jerry et al., 2017; Mulaosmanovic et al., 2017; Mulaosmanovic et al., 2018; Ni et al., 2018; Dutta et al., 2019). They have been reported to mimic synaptic behavior and key neuronal functions. In particular, HfO_2-based FeFETs with analog threshold voltage (Mulaosmanovic et al., 2017) (V_t) and channel conductance tuning (Jerry et al., 2017; Ni et al., 2018) have been employed in synaptic applications as well as leaky integrate-and-fire (LIF) neuron models (Mulaosmanovic et al., 2018; Dutta et al., 2019). These neuromorphic applications have been realized through the partial polarization domain switching in ferroelectric HfO_2 thin films (Jerry et al., 2017; Ni et al., 2018). HfO_2-based ferroelectrics have been applied in ferroelectric tunnel junctions (FTJs) (Chen et al., 2018; Kobayashi et al., 2018; Cheema et al., 2020; Goh et al., 2020; Ma et al., 2020), negative capacitance field-effect transistors (NCFETs) (Hoffmann et al., 2016; Si et al., 2018; Kim et al., 2019), sensors (Smith et al., 2017; Jachalke et al., 2018; Mart et al., 2018), and energy storage (Ali et al., 2017; Kühnel et al., 2019) and conversion (Hoffmann et al., 2015). A high remnant polarization ($2P_r$) of the ferroelectric thin films that can sustain numerous switching cycles without degradation generally benefits memory applications such as FeRAMs (Kondo et al., 2007; Park et al., 2018b). However, a high remnant polarization is detrimental for FeFET and FTJ applications due to the highly concentrated electric field in the interfacial layers resulting from the high depolarization field in the ferroelectric layer. Nevertheless, large $2P_r$ not only reflects high asymmetric ionic displacement from the center of mass and higher nonvolatile charge density in the capacitor, but also indicates microstructural uniformity in the HfO_2-based ferroelectrics.

Doping HfO_2 with elements such as silicon (Böscke et al., 2011; Mart et al., 2018; Kühnel et al., 2019), aluminum (Mueller et al., 2012b; Müller et al., 2013; Zhou et al., 2020), gadolinium (Mueller et al., 2012a; Sang et al., 2015), zirconium (Zr) (Karbasian et al., 2017; Smith et al., 2017; Chen et al., 2018; Francois et al., 2019; Kim et al., 2019; Zacharaki et al., 2019; Goh et al., 2020; Okuno et al., 2020; Kashir et al., 2021), lanthanum (La) (Chernikova et al., 2018; Schroeder et al., 2018; Kozodaev et al., 2019; Song et al., 2020), etc., has been proven to improve its ferroelectric polarization by stabilizing the non-centrosymmetric orthorhombic phase ($Pca2_1$). Among others, zirconium has been shown to be a very effective dopant at ~50 cat% concentration because it reduces the crystallization temperature and improves the ferroelectric properties of HfO_2. Additionally, HfO_2-ZrO_2 solid solution has a wider Zr concentration range for favoring the ferroelectric phase compared to other dopants. This system is commonly referred to as hafnium zirconium oxide (HZO). Electrode materials sandwiching the ferroelectric film has also been found to play a role in stabilizing the orthorhombic phase (*o*-phase) (Karbasian et al., 2017; Goh et al., 2020). Although titanium nitride (TiN) is the most widely used electrode, it was recently reported that materials like tungsten (W) (Goh et al., 2020) with a relatively low thermal expansion coefficient ($\alpha_W = 4.5 \times 10^{-6}$ °C^{-1}, $\alpha_{TiN} = 9.4 \times 10^{-6}$ °C^{-1}) improved remnant polarization by suppressing the formation of the monoclinic phase (*m*-phase).

In this work, the influence of varying rapid thermal annealing (RTA) temperatures after top electrode (TE) deposition on the $2P_r$ of W/HZO/W ferroelectric capacitors was investigated. To stabilize large ferroelectricity, an appreciable tensile stress was induced during RTA by sandwiching HZO with W electrodes. A record-high $2P_r$ was achieved with the capacitors operated at a particularly high frequency of 111 kHz. These HZO capacitors endured 10^8 positive-up-negative-down (PUND) cycles while exhibiting a high $2P_r$. Finally, a promising polarization retention was observed at various temperatures (25, 85, and 125°C) with very little polarization degradation over the monitored duration of 10^3 min.

Materials and methods

To fabricate the capacitors, a ~10 nm HZO film was deposited on the bottom electrode (BE) via the atomic layer deposition (ALD) process at 200°C, with tetrakis (dimethylamino)hafnium (TDMA–Hf) and tetrakis (dimethylamino)zirconium (TDMA–Zr) as the Hf and Zr precursors, respectively, and water (H_2O) as the oxidant. To maintain the Hf:Zr ratio as close to 1:1 as possible, each cycle consisted of one sub-cycle of TDMA–Hf and H_2O, and another sub-cycle of TDMA–Zr and H_2O.

For the BE, a blanket thin film of 70-nm thick W was sputter-coated on a silicon wafer with a 300 nm SiO_2 layer grown thermally. Another 45-nm thick W layer was sputter-deposited as the TE and a 50-nm thick platinum (Pt) was used to cap-off the capacitors. A device with a size of 30 µm × 30 µm was defined by TE pads patterned via photolithography and liftoff processes. The capacitors were then subjected to RTA for 1 min with five different annealing temperatures (400, 500, 600, 700, and 800°C) under the nitrogen atmosphere. All electrical characterization tests were performed using Keysight's B1530A waveform generator/fast measurement unit module at room temperature (25°C).

Results and discussion

The ferroelectric hysteresis curves of the capacitors were obtained using a PUND voltage scheme with triangular pulses at 100 kHz frequency and a voltage amplitude of 4 V. The HZO capacitors were first woken up by using one million trapezoidal PUND pulse cycles with an amplitude of 4 V at a frequency of 111 kHz before obtaining the polarization data in **Figure 1A**. The capacitors annealed at 500 and 600°C exhibited a $2P_r$ of about 42 μC cm^{-2} and 57 μC cm^{-2}, respectively. In particular, the capacitors annealed at 700°C resulted in a $2P_r$ of ∼64 μC cm^{-2}, which is among the largest reported values and the highest ever achieved at such a high frequency of 100 kHz. **Figure 1B** shows the bar plot of how $2P_r$ of the capacitors increased with an increase in RTA temperature. This could be attributed to an enhanced formation of polar *o*-phase and a greater ferroelectric polarization at higher RTA temperatures (Fig. **Supplementary Figure S1**) (Kashir et al., 2021). In addition, previous studies have demonstrated that the *m*-phase, which is responsible for attenuating ferroelectricity, can almost entirely be suppressed at high annealing temperatures (Pal et al., 2017; Park et al., 2018a; Kashir et al., 2021). These phenomena might be the reasons why the capacitors annealed at 700°C have shown such a large $2P_r$. However, when annealed at 800°C, the capacitors became highly leaky and shorted when a voltage greater than 1 V was applied. A possible explanation for this could be the excessive amount of oxygen vacancies generated in the HZO through oxygen scavenging by the W electrodes during annealing (Lomenzo et al., 2016; Pešić et al., 2016; Kashir et al., 2021). On the other hand, HZO capacitors annealed at 400°C did not display any ferroelectric behavior, even after annealing at the same temperature twice (**Supplementary Figure S2**). A low deposition temperature of 200°C coupled with weak oxidant like water is known to facilitate increased carbon impurity in HZO thin films, which may have resulted in the late appearance of ferroelectricity (from 500°C onwards) (Materano et al., 2020; Hsain et al., 2022).

Ferroelectric hysteresis measurement using a dynamic hysteresis mode (DHM) can lead to an overestimation of the polarization charge. That is, the bipolar triangle pulses applied with a delay in between two excitations in DHM do not account for the non-ferroelectric contributions accumulated along with the ferroelectric component. The PUND technique, however, was designed to cancel out such non-ferroelectric contributions (Scott et al., 1988). Although this method can almost truly extract the ferroelectric contribution, it still fails to eliminate

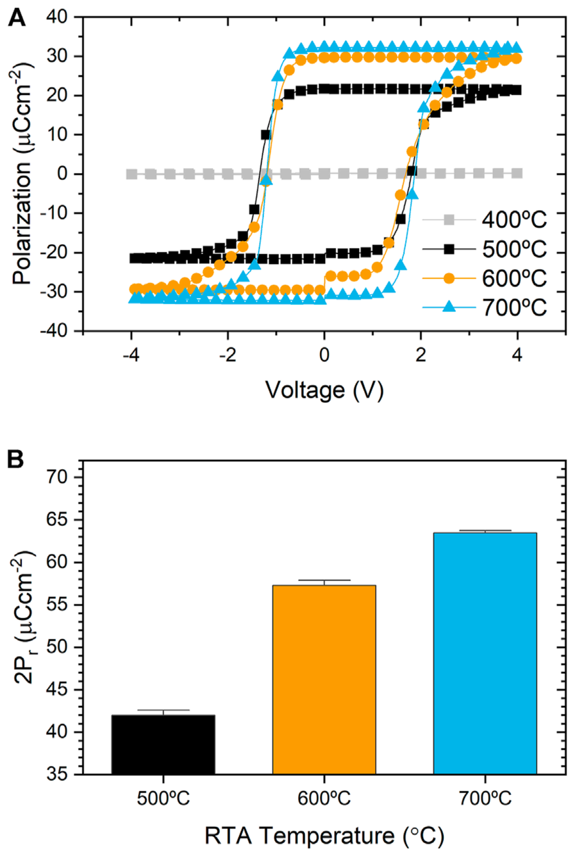

FIGURE 1
(A) Polarization-voltage plots of HZO capacitors annealed at various temperatures obtained using triangular PUND voltage scheme at 100 kHz. **(B)** Variation of $2P_r$ with respect to RTA temperature. The error bars represent standard deviation.

leakage current in the low-frequency regime (Fina et al., 2011). Therefore, the higher the frequency of the pulse scheme used, the closer the results are to the true ferroelectric polarization values. A clear trend of the remnant polarization is presented in **Figure 2A**, wherein the $2P_r$ value decreased as the frequency of the PUND scheme increased for all the measured HZO capacitors. For example, the average $2P_r$ of capacitors annealed at 700°C is 87.6 ± 5.1 μC cm^{-2} at 1 kHz. This value was reduced to 71.3 ± 0.6 μC cm^{-2} at 10 kHz and further decreased to 63.0 ± 0.1 μC cm^{-2} at 100 kHz. Evidently, the values at lower frequencies revealed a larger spread, indicating the presence of leakage contributions. In **Figure 2B**, the same observation is shown in terms of polarization-voltage hysteresis curves. As the frequency decreased, the loop opened, and the curves became rounded around ±4 V.

To characterize the endurance of all three HZO capacitors with meaningful $2P_r$, a PUND voltage scheme with trapezoidal pulses of 1.5 μs width, rise and fall times of 1.5 μs each (i.e., frequency of 111 kHz), and a voltage of ±4 V was employed

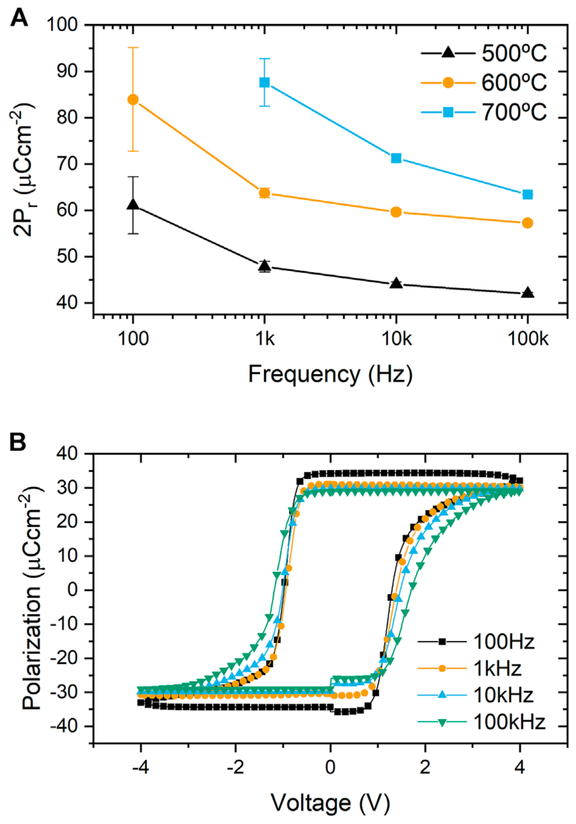

FIGURE 2
(A) Dependence of $2P_r$ on the frequency of PUND scheme. **(B)** Polarization-voltage plots obtained using different frequencies of PUND scheme in HZO capacitors annealed at 600°C.

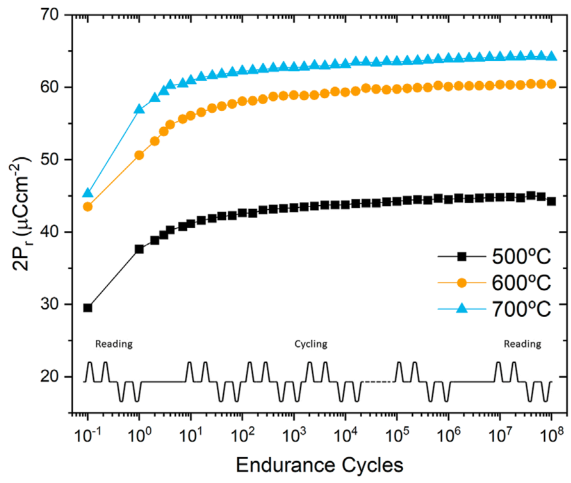

FIGURE 3
Endurance tests of the different HZO capacitors performed using trapezoidal PUND pulses with an amplitude 4 V and a frequency of 111 kHz frequency (i.e., t_r = t_f = 1.5 μs, t_h = 1.5 μs).

for both cycling and measuring 2Pr as shown in the inset of **Figure 3**. The $2P_r$ value was measured five times for every decade of endurance cycles, as plotted in **Figure 3**. A jump in $2P_r$ was observed from the pristine cycle (data points plotted at 10^{-1} of the endurance cycles axis) to the first cycle in all three cases. The jumps were ~8 μC cm^{-2}, ~7 μC cm^{-2}, and ~11 μC cm^{-2} for capacitors annealed at 500, 600, and 700°C, respectively. After this initial jump, the $2P_r$ value started to increase steadily. This observation is due to the wake-up effect generally seen in HZO-based ferroelectrics (Mehmood et al., 2020; Jiang et al., 2021) and even in traditional ferroelectrics like lead zirconate titanate (Carl and Hardtl, 1977). In the case of the capacitors annealed at 500°C, $2P_r$ increased to ~43 μC cm^{-2} (95.5%) after just 100 cycles. Similarly, after 100 cycles, $2P_r$ of capacitors annealed at 600 and 700°C increased to ~58 μC cm^{-2} (96.0%) and ~62 μC cm^{-2} (96.5%), respectively. These results reveal commendable wake-up behavior in all three HZO capacitors. We believe that these findings could be attributed to the large electric field (4 MVcm^{-1}) used during the endurance tests, which is known to accelerate the number of cycles required for wake-up (Zhou et al., 2013).

Remarkably, the capacitors annealed at 700°C maintained a large $2P_r$ of ~64 μC cm^{-2} without detectable fatigue or breakdown, even after 10^8 cycles under such relatively large cycling voltage. The capacitors annealed at 600°C also exhibited a comparable endurance performance with ~60 μC cm^{-2} remnant polarization. However, the capacitors annealed at 500°C showed an onset of fatigue after ~6.3×10^7 cycles. The use of high frequency cycling could have resulted in improved endurance behavior while exhibiting such high $2P_r$ (Liao et al., 2021). These results are encouraging, as previous studies reported either a high $2P_r$ value with a low endurance (Schroeder et al., 2018; Zacharaki et al., 2019; Kashir et al., 2021) or a high endurance with a low $2P_r$ value (Chernikova et al., 2018; Kozodaev et al., 2019).

To further probe the endurance of fabricated HZO capacitors, voltage pulses with an amplitude of ±1.5 V were applied at a frequency of 1.67 MHz for 10^{10} cycles (**Supplementary Figure S3**). Under these test parameters, all three capacitors manifested a lower $2P_r$ value that started declining at around 10^7 and 10^8 cycles. Lower $2P_r$ values were obtained because the applied voltage amplitude was not sufficient to achieve a complete polarization switching of all the available domains. This phenomenon is referred to as unsaturated polarization switching or subcycling behavior (Schenk et al., 2014; Li et al., 2020). The decline in the $2P_r$ can also be attributed to the subcycling effect where the domains segregate into groups that require different voltages for switching. Subcycling is more pronounced at reduced cycling voltages and higher frequencies (Li et al., 2020). On the other hand, the application of larger voltages at such high frequencies resulted in the premature breakdown of the capacitors. Nonetheless, all

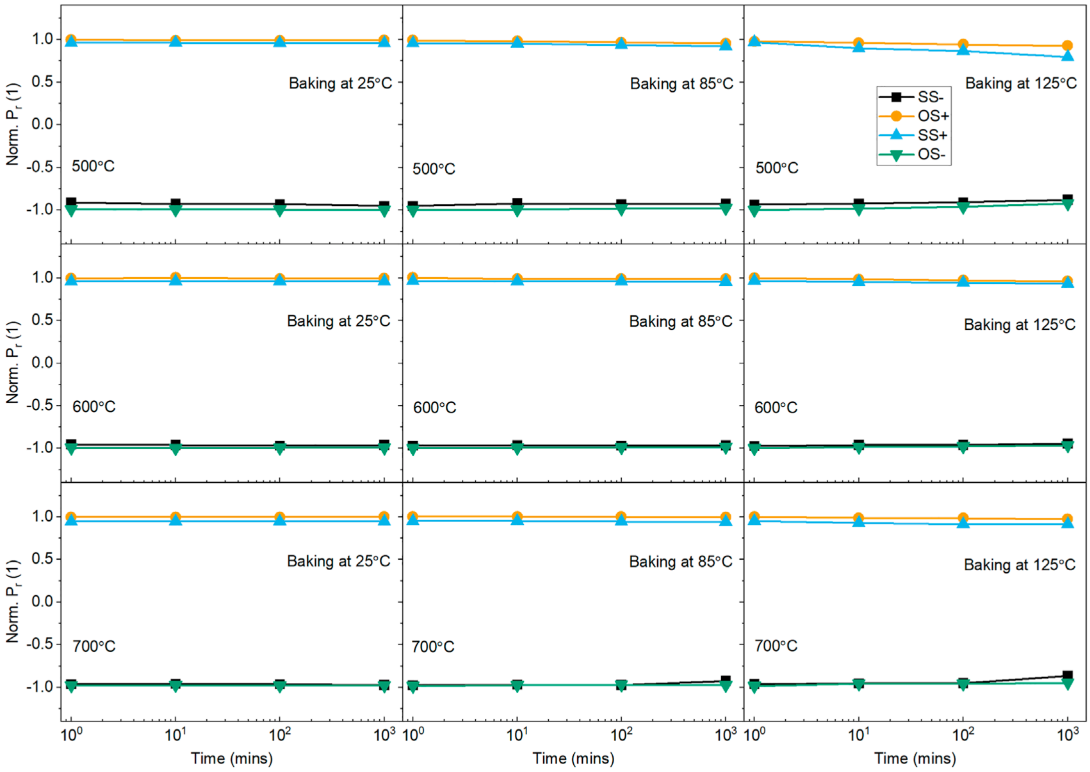

FIGURE 4
Retention tests of the different HZO capacitors performed at 25, 85, and 125°C.

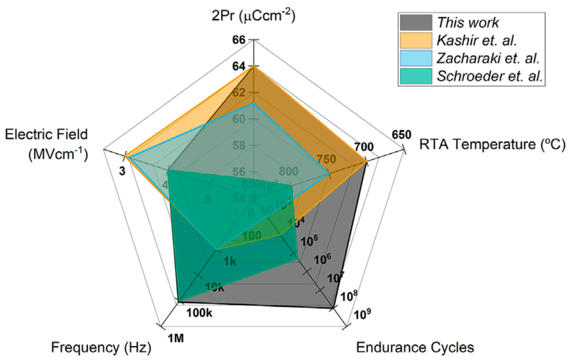

FIGURE 5
Performance comparison of this study with other works (Schroeder et al., 2018; Zacharaki et al., 2019; Kashir et al., 2021) with high 2P_r.

capacitors were still switchable after 10^{10} cycles, even under a fast-testing mode.

To further characterize the reliability of the HZO capacitors, retention tests were conducted at different temperatures (25, 85, and 125 °C) with baking times of 1, 10, 100, and 1,000 min. The capacitors were cooled down to room temperature (25°C) for read and write operations. Two pulse waveforms (PUND and NDPU) with a voltage amplitude of ±4 V at 111 kHz were applied to measure the retention of the same state (SS+ and SS-) and opposite state (OS+ and OS-) polarization. Five million PUND cycles, also with ±4 V at 111 kHz, were used at room temperature (25°C) to fully wake-up the capacitors before starting the retention tests. **Figure 4** shows the results of the retention tests on six capacitors (2 capacitors each for the three RTA temperatures) where the polarization monitored was normalized. One capacitor was subjected to PUND pulse waveform to monitor SS+ and OS- polarization whereas the other was subjected to NDPU pulse waveform to monitor SS- and OS+ polarization. Details of the retention measurement procedure can be found in **Supplementary Figure S4**. In most cases, no discernible retention loss was observed, which is most likely due to the polarization states being close to full saturation (Mueller et al., 2012c). However, a small retention loss was detected in the capacitors annealed at 500°C, which may be attributed to a larger depolarization field in the HZO thin film. This field results from a greater proportion of the non-polar tetragonal phase formed at such a lower annealing temperature (Mehmood et al., 2019). Although the HZO capacitors suffered from imprint (**Supplementary Figure S5**), the findings from the retention tests hold great potential for neuromorphic computing applications.

To compare the performance of fabricated HZO capacitors with previous literature featuring large $2P_r$ values in doped HfO_2 capacitors after RTA, a radar chart showing the impact of various experimental conditions was generated, as shown in **Figure 5**. Generally, the values of each parameter increase from the center towards the perimeter of the chart. However, the electric field ($MVcm^{-1}$) and RTA temperature (°C) axes were inverted so that the desirable values are located towards the edge, just like other performance parameters. In other words, a low operating voltage and thermal budget are desired. In their recently published work, Kashir et al. (2021) reported a similar $2P_r$ of ~ 64 μC cm^{-2} while annealing the HZO capacitors at 700°C for 5 s. Employing a 3 V - 1 kHz triangular pulse PUND technique for the endurance tests, they were only able to achieve a maximum of 10^4 cycles before encountering breakdown. To improve the leakage behavior of their HZO capacitor, they inserted a Pt layer between the W and HZO interface, which increased the potential barrier and resulted in a lower current density. Zacharaki et al. (2019) utilized an epitaxial HZO thin film grown on germanium to achieve a $2P_r$ of 61.2 μC cm^{-2}. Despite a promising achievement, they were only able to cycle their epitaxial HZO capacitors for 10^3 cycles, after which the leakage current increased significantly and resulted in a device breakdown. Their best endurance was reported to be over 10^5 cycles with a reduced $2P_r$ at ~ 40 μC cm^{-2} under an electric field of 2.3$MVcm^{-1}$ Schroeder et al. (2018) reported decent endurance results at 10^9 cycles in lanthanum-doped hafnia (HLO) with a La concentration of over 10 cat% but with a trade-off in $2P_r$. After performing RTA at 800°C, their HLO capacitors with a maximum $2P_r$ of 55.4 μC cm^{-2} were able to achieve 2×10^5 endurance cycles at 4 V - 100 kHz. Remarkably, the fabricated HZO capacitors in this work, specifically those which were annealed at 700°C, have either performed similarly or outperformed the previous works with better endurance while preserving a large $2P_r$ for the endurance measurements performed at 111 kHz frequency.

Conclusion

In summary, our fabricated HZO-based ferroelectric capacitors demonstrated a $2P_r$ value as high as 64 μC cm^{-2}, an endurance of 100 million cycles, and promising retention performance. We discovered that the $2P_r$ value increased with the RTA temperature up to 700°C. We also emphasized that the frequency of the applied PUND voltage scheme in measuring the polarization is crucial to avoid overestimated results. Our HZO ferroelectric films with a large remnant polarization and great reliability characteristics can potentially be used to engineer both synaptic and neuronal devices for neuromorphic computing applications.

Data availability statement

The original contributions presented in the study are included in the article/**Supplementary Material**, further inquiries can be directed to the corresponding authors.

Author contributions

JY conceived the concept. JY, YC, and SA designed the experiments. SA fabricated the devices and performed electrical and X-ray characterizations. JP carried out RTA. YZ wrote a custom code for endurance and retention measurements. TM, RM, DG, JL, QW, MB, SG, RK, YC, QX, and JY helped with experiments and data analysis. SA, JP, JY, YC, and RK prepared, reviewed and edited the manuscript. All the authors participated in discussing the results and commented on the manuscript at every stage.

Funding

This work was partially supported by the Air Force Office of Scientific Research (AFOSR) through the Multidisciplinary University Research Initiative (MURI) program under contract no. FA9550-19-1-0213 and the United States Air Force Research Laboratory (AFRL) under grant no. FA8750-18-2-0122 and FA8650-21-C-5405. This work was also partially supported by the National Science Foundation under contract no. 2023752. The opinions, findings, and conclusion, or recommendation expressed in this material are those of the authors and do not necessarily reflect the views of AFRL.

Acknowledgments

RK appreciates the faculty start-up fund from UMass Amherst.

Conflict of interest

The authors declare that the research was conducted in the absence of any commercial or financial relationships that could be construed as a potential conflict of interest.

Publisher's note

All claims expressed in this article are solely those of the authors and do not necessarily represent those of their affiliated organizations, or those of the publisher, the editors and the reviewers. Any product that may be evaluated in this article, or claim that may be made by its manufacturer, is not guaranteed or endorsed by the publisher.

Supplementary material

The Supplementary Material for this article can be found online at: https://www.frontiersin.org/articles/10.3389/fmats.2022.969188/full#supplementary-material

References

Ali, F., Liu, X., Zhou, D., Yang, X., Xu, J., Schenk, T., et al. (2017). Silicon-doped hafnium oxide anti-ferroelectric thin films for energy storage. *J. Appl. Phys.* 122, 144105. doi:10.1063/1.4989908

Böscke, T., Müller, J., Bräuhaus, D., Schröder, U., and Böttger, U. (2011). Ferroelectricity in hafnium oxide thin films. *Appl. Phys. Lett.* 99, 102903. doi:10.1063/1.3634052

Carl, K., and Hardtl, K. (1977). Electrical after-effects in $Pb(Ti,Zr)O_3$ ceramics. *Ferroelectrics* 17, 473–486. doi:10.1080/00150197808236770

Cheema, S. S., Kwon, D., Shanker, N., Dos Reis, R., Hsu, S.-L., Xiao, J., et al. (2020). Enhanced ferroelectricity in ultrathin films grown directly on silicon. *Nature* 580, 478–482. doi:10.1038/s41586-020-2208-x

Chen, L., Wang, T.-Y., Dai, Y.-W., Cha, M.-Y., Zhu, H., Sun, Q.-Q., et al. (2018). Ultra-low power $Hf_{0.5}Zr_{0.5}O_2$ based ferroelectric tunnel junction synapses for hardware neural network applications. *Nanoscale* 10, 15826–15833. doi:10.1039/c8nr04734k

Chernikova, A. G., Kozodaev, M. G., Negrov, D. V., Korostylev, E. V., Park, M. H., Schroeder, U., et al. (2018). Improved ferroelectric switching endurance of La-doped $Hf_{0.5}Zr_{0.5}O_2$ thin films. *ACS Appl. Mat. Interfaces* 10, 2701–2708. doi:10.1021/acsami.7b15110

Dünkel, S., Trentzsch, M., Richter, R., Moll, P., Fuchs, C., Gehring, O., et al. (2017). "A FEFET based super-low-power ultra-fast embedded NVM technology for 22nm FDSOI and beyond," in 2017 IEEE International Electron Devices Meeting (IEDM), San Francisco, CA, USA, 02-06 December 2017 (IEEE), 19–27.

Dutta, S., Saha, A., Panda, P., Chakraborty, W., Gomez, J., Khanna, A., et al. (2019). "Biologically plausible ferroelectric quasi-leaky integrate and fire neuron," in 2019 Symposium on VLSI Technology, Kyoto, Japan, 09-14 June 2019 (IEEE), T140–T141.

Dutta, S., Ye, H., Chakraborty, W., Luo, Y.-C., San Jose, M., Grisafe, B., et al. (2020). "Monolithic 3D integration of high endurance multi-bit ferroelectric fet for accelerating compute-in-memory," in 2020 IEEE International Electron Devices Meeting (IEDM), San Francisco, CA, USA, 12-18 December 2020 (IEEE), 36–44.

Fina, I., Fàbrega, L., Langenberg, E., Martí, X., Sánchez, F., Varela, M., et al. (2011). Nonferroelectric contributions to the hysteresis cycles in manganite thin films: A comparative study of measurement techniques. *J. Appl. Phys.* 109, 074105. doi:10.1063/1.3555098

Francois, T., Grenouillet, L., Coignus, J., Blaise, P., Carabasse, C., Vaxelaire, N., et al. (2019). "Demonstration of BEOL-compatible ferroelectric $Hf_{0.5}Zr_{0.5}O_2$ scaled feram co-integrated with 130nm CMOS for embedded nvm applications," in 2019 IEEE International Electron Devices Meeting (IEDM), San Francisco, CA, USA, 07-11 December 2019 (IEEE), 15–17.

George, S., Ma, K., Aziz, A., Li, X., Khan, A., Salahuddin, S., et al. (2016). "Nonvolatile memory design based on ferroelectric FETs," in 2016 53nd ACM/EDAC/IEEE Design Automation Conference (DAC), Austin, TX, USA, 05-09 June 2016 (IEEE), 1–6.

Goh, Y., Hwang, J., Lee, Y., Kim, M., and Jeon, S. (2020). Ultra-thin $Hf_{0.5}Zr_{0.5}O_2$ thin-film-based ferroelectric tunnel junction via stress induced crystallization. *Appl. Phys. Lett.* 117, 242901. doi:10.1063/5.0029516

Hoffmann, M., Pešić, M., Chatterjee, K., Khan, A. I., Salahuddin, S., Slesazeck, S., et al. (2016). Direct observation of negative capacitance in polycrystalline ferroelectric HfO_2. *Adv. Funct. Mat.* 26, 8643–8649. doi:10.1002/adfm.201602869

Hoffmann, M., Schroeder, U., Künneth, C., Kersch, A., Starschich, S., Böttger, U., et al. (2015). Ferroelectric phase transitions in nanoscale HfO_2 films enable giant pyroelectric energy conversion and highly efficient supercapacitors. *Nano Energy* 18, 154–164. doi:10.1016/j.nanoen.2015.10.005

Hsain, H. A., Lee, Y., Materano, M., Mittmann, T., Payne, A., Mikolajick, T., et al. (2022). Many routes to ferroelectric HfO_2: A review of current deposition methods. *J. Vac. Sci. Technol. A* 40, 010803. doi:10.1116/6.0001317

Jachalke, S., Schenk, T., Park, M. H., Schroeder, U., Mikolajick, T., Stöcker, H., et al. (2018). Pyroelectricity of silicon-doped hafnium oxide thin films. *Appl. Phys. Lett.* 112, 142901. doi:10.1063/1.5023390

Jerry, M., Chen, P.-Y., Zhang, J., Sharma, P., Ni, K., Yu, S., et al. (2017). "Ferroelectric FET analog synapse for acceleration of deep neural network training," in 2017 IEEE International Electron Devices Meeting (IEDM), San Francisco, CA, USA, 02-06 December 2017 (IEEE), 6–2.

Jiang, P., Luo, Q., Xu, X., Gong, T., Yuan, P., Wang, Y., et al. (2021). Wake-up effect in HfO_2-based ferroelectric films. *Adv. Electron. Mat.* 7, 2000728. doi:10.1002/aelm.202000728

Karbasian, G., Dos Reis, R., Yadav, A. K., Tan, A. J., Hu, C., Salahuddin, S., et al. (2017). Stabilization of ferroelectric phase in tungsten capped $Hf_{0.8}Zr_{0.2}O_2$. *Appl. Phys. Lett.* 111, 022907. doi:10.1063/1.4993739

Kashir, A., Kim, H., Oh, S., and Hwang, H. (2021). Large remnant polarization in a wake-up free $Hf_{0.5}Zr_{0.5}O_2$ ferroelectric film through bulk and interface engineering. *ACS Appl. Electron. Mat.* 3, 629–638. doi:10.1021/acsaelm.0c00671

Kim, K. D., Kim, Y. J., Park, M. H., Park, H. W., Kwon, Y. J., Lee, Y. B., et al. (2019). Transient negative capacitance effect in atomic-layer-deposited $Al_2O_3/Hf_{0.3}Zr_{0.7}O_2$ bilayer thin film. *Adv. Funct. Mat.* 29, 1808228. doi:10.1002/adfm.201808228

Kobayashi, M., Tagawa, Y., Mo, F., Saraya, T., and Hiramoto, T. (2018). Ferroelectric HfO_2 tunnel junction memory with high ter and multi-level operation featuring metal replacement process. *IEEE J. Electron Devices Soc.* 7, 134–139. doi:10.1109/jeds.2018.2885932

Kondo, V., Singh, V. S. K., and Ishiwara, V. H. (2007). New ferroelectric material for embedded fram LSIs. *Fujitsu Sci. Tech. J.* 43, 502–507.

Kozodaev, M. G., Chernikova, A. G., Korostylev, E. V., Park, M. H., Khakimov, R. R., Hwang, C. S., et al. (2019). Mitigating wakeup effect and improving endurance of ferroelectric HfO_2-ZrO_2 thin films by careful la-doping. *J. Appl. Phys.* 125, 034101. doi:10.1063/1.5050700

Kühnel, K., Czernohorsky, M., Mart, C., and Weinreich, W. (2019). High-density energy storage in Si-doped hafnium oxide thin films on area-enhanced substrates. *J. Vac. Sci. Technol. B* 37, 021401. doi:10.1116/1.5060738

Li, S., Zhou, D., Shi, Z., Hoffmann, M., Mikolajick, T., Schroeder, U., et al. (2020). Involvement of unsaturated switching in the endurance cycling of Si-doped HfO_2 ferroelectric thin films. *Adv. Electron. Mat.* 6, 2000264. doi:10.1002/aelm.202000264

Liao, P., Chang, Y., Lee, Y.-H., Lin, Y., Yeong, S., Hwang, R., et al. (2021). "Characterization of fatigue and its recovery behavior in ferroelectric HfZrO," in 2021 Symposium on VLSI Technology, Kyoto, Japan, 13-19 June 2021 (IEEE), 1–2.

Lomenzo, P. D., Takmeel, Q., Moghaddam, S., and Nishida, T. (2016). Annealing behavior of ferroelectric Si-doped HfO_2 thin films. *Thin Solid Films* 615, 139–144. doi:10.1016/j.tsf.2016.07.009

Ma, C., Luo, Z., Huang, W., Zhao, L., Chen, Q., Lin, Y., et al. (2020). Sub-nanosecond memristor based on ferroelectric tunnel junction. *Nat. Commun.* 11, 1439. doi:10.1038/s41467-020-15249-1

Mart, C., Kämpfe, T., Zybell, S., and Weinreich, W. (2018). Layer thickness scaling and wake-up effect of pyroelectric response in Si-doped HfO_2. *Appl. Phys. Lett.* 112, 052905. doi:10.1063/1.5019308

Materano, M., Richter, C., Mikolajick, T., and Schroeder, U. (2020). $Hf_xZr_{1-x}O_2$ thin films for semiconductor applications: An hf-and zr-ald precursor comparison. *J. Vac. Sci. Technol. A* 38, 022402. doi:10.1116/1.5134135

Mehmood, F., Hoffmann, M., Lomenzo, P. D., Richter, C., Materano, M., Mikolajick, T., et al. (2019). Bulk depolarization fields as a major contributor to the ferroelectric reliability performance in lanthanum doped $Hf_{0.5}Zr_{0.5}O_2$ capacitors. *Adv. Mat. Interfaces* 6, 1901180. doi:10.1002/admi.201901180

Mehmood, F., Mikolajick, T., and Schroeder, U. (2020). Wake-up mechanisms in ferroelectric lanthanum-doped $Hf_{0.5}Zr_{0.5}O_2$ thin films. *Phys. Status Solidi A* 217, 2000281. doi:10.1002/pssa.202000281

Mueller, S., Adelmann, C., Singh, A., Van Elshocht, S., Schroeder, U., Mikolajick, T., et al. (2012a). Ferroelectricity in Gd-doped HfO_2 thin films. *ECS J. Solid State Sci. Technol.* 1, N123–N126. doi:10.1149/2.002301jss

Mueller, S., Mueller, J., Singh, A., Riedel, S., Sundqvist, J., Schroeder, U., et al. (2012b). Incipient ferroelectricity in Al-doped HfO_2 thin films. *Adv. Funct. Mat.* 22, 2412–2417. doi:10.1002/adfm.201103119

Mueller, S., Muller, J., Schroeder, U., and Mikolajick, T. (2012c). Reliability characteristics of ferroelectric Si:HfO_2 thin films for memory applications. *IEEE Trans. Device Mat. Reliab.* 13, 93–97. doi:10.1109/tdmr.2012.2216269

Mulaosmanovic, H., Chicca, E., Bertele, M., Mikolajick, T., and Slesazeck, S. (2018). Mimicking biological neurons with a nanoscale ferroelectric transistor. *Nanoscale* 10, 21755–21763. doi:10.1039/c8nr07135g

Mulaosmanovic, H., Ocker, J., Müller, S., Noack, M., Müller, J., Polakowski, P., et al. (2017). "Novel ferroelectric fet based synapse for neuromorphic systems," in 2017 Symposium on VLSI Technology, Kyoto, Japan, 05-08 June 2017 (IEEE), T176–T177.

Müller, J., Böscke, T., Müller, S., Yurchuk, E., Polakowski, P., Paul, J., et al. (2013). "Ferroelectric hafnium oxide: A CMOS-compatible and highly scalable approach to future ferroelectric memories," in 2013 IEEE International Electron Devices Meeting, Washington, DC, USA, 09-11 December 2013 (IEEE), 10–18.

Ni, K., Smith, J., Grisafe, B., Rakshit, T., Obradovic, B., Kittl, J., et al. (2018). "SoC logic compatible multi-bit femfet weight cell for neuromorphic applications," in 2018 IEEE International Electron Devices Meeting (IEDM), San Francisco, CA, USA, 01-05 December 2018 (IEEE), 13–22.

Okuno, J., Kunihiro, T., Konishi, K., Maemura, H., Shute, Y., Sugaya, F., et al. (2020). "SoC compatible 1T1C FERAM memory array based on ferroelectric $Hf_{0.5}Zr_{0.5}O_2$," in 2020 IEEE Symposium on VLSI Technology, Honolulu, HI, USA, 16-19 June 2020 (IEEE), 1–2.

Pal, A., Narasimhan, V. K., Weeks, S., Littau, K., Pramanik, D., Chiang, T., et al. (2017). Enhancing ferroelectricity in dopant-free hafnium oxide. *Appl. Phys. Lett.* 110, 022903. doi:10.1063/1.4973928

Park, M. H., Chung, C.-C., Schenk, T., Richter, C., Opsomer, K., Detavernier, C., et al. (2018a). Effect of annealing ferroelectric HfO_2 thin films: *In situ*, high temperature X-ray diffraction. *Adv. Electron. Mat.* 4, 1800091. doi:10.1002/aelm.201800091

Park, M. H., Lee, Y. H., Mikolajick, T., Schroeder, U., and Hwang, C. S. (2018b). Review and perspective on ferroelectric HfO_2-based thin films for memory applications. *MRS Commun.* 8, 795–808. doi:10.1557/mrc.2018.175

Pešić, M., Fengler, F. P. G., Larcher, L., Padovani, A., Schenk, T., Grimley, E. D., et al. (2016). Physical mechanisms behind the field-cycling behavior of HfO_2-based ferroelectric capacitors. *Adv. Funct. Mat.* 26, 4601–4612. doi:10.1002/adfm.201600590

Sang, X., Grimley, E. D., Schenk, T., Schroeder, U., and LeBeau, J. M. (2015). On the structural origins of ferroelectricity in HfO_2 thin films. *Appl. Phys. Lett.* 106, 162905. doi:10.1063/1.4919135

Schenk, T., Schroeder, U., Pesic, M., Popovici, M., Pershin, Y. V., Mikolajick, T., et al. (2014). Electric field cycling behavior of ferroelectric hafnium oxide. *ACS Appl. Mat. Interfaces* 6, 19744–19751. doi:10.1021/am504837r

Schroeder, U., Richter, C., Park, M. H., Schenk, T., Pesic, M., Hoffmann, M., et al. (2018). Lanthanum-doped hafnium oxide: A robust ferroelectric material. *Inorg. Chem.* 57, 2752–2765. doi:10.1021/acs.inorgchem.7b03149

Scott, J. F., Kammerdiner, L., Parris, M., Traynor, S., Ottenbacher, V., Shawabkeh, A., et al. (1988). Switching kinetics of lead zirconate titanate submicron thin-film memories. *J. Appl. Phys.* 64, 787–792. doi:10.1063/1.341925

Si, M., Su, C.-J., Jiang, C., Conrad, N. J., Zhou, H., Maize, K. D., et al. (2018). Steep-slope hysteresis-free negative capacitance MoS_2 transistors. *Nat. Nanotechnol.* 13, 24–28. doi:10.1038/s41565-017-0010-1

Smith, S., Kitahara, A., Rodriguez, M., Henry, M., Brumbach, M., Ihlefeld, J., et al. (2017). Pyroelectric response in crystalline hafnium zirconium oxide ($Hf_{1-x}Zr_xO_2$) thin films. *Appl. Phys. Lett.* 110, 072901. doi:10.1063/1.4976519

Song, T., Bachelet, R., Saint-Girons, G., Solanas, R., Fina, I., Sánchez, F., et al. (2020). Epitaxial ferroelectric La-doped $Hf_{0.5}Zr_{0.5}O_2$ thin films. *ACS Appl. Electron. Mat.* 2, 3221–3232. doi:10.1021/acsaelm.0c00560

Zacharaki, C., Tsipas, P., Chaitoglou, S., Fragkos, S., Axiotis, M., Lagoyiannis, A., et al. (2019). Very large remanent polarization in ferroelectric $Hf_{1-x}Zr_xO_2$ grown on ge substrates by plasma assisted atomic oxygen deposition. *Appl. Phys. Lett.* 114, 112901. doi:10.1063/1.5090036

Zhou, D., Xu, J., Li, Q., Guan, Y., Cao, F., Dong, X., et al. (2013). Wake-up effects in Si-doped hafnium oxide ferroelectric thin films. *Appl. Phys. Lett.* 103, 192904. doi:10.1063/1.4829064

Zhou, J., Zhou, Z., Wang, X., Wang, H., Sun, C., Han, K., et al. (2020). Demonstration of ferroelectricity in Al-doped HfO_2 with a low thermal budget of 500°C. *IEEE Electron Device Lett.* 41, 1130–1133.